

Supplementary Materials for

**South Asian summer monsoon enhanced by the uplift of Iranian Plateau in
Middle Miocene**

1. Vegetation maps
2. Moisture budget decomposition
3. Geographic sensitivity Experiments

SM1: Vegetation maps

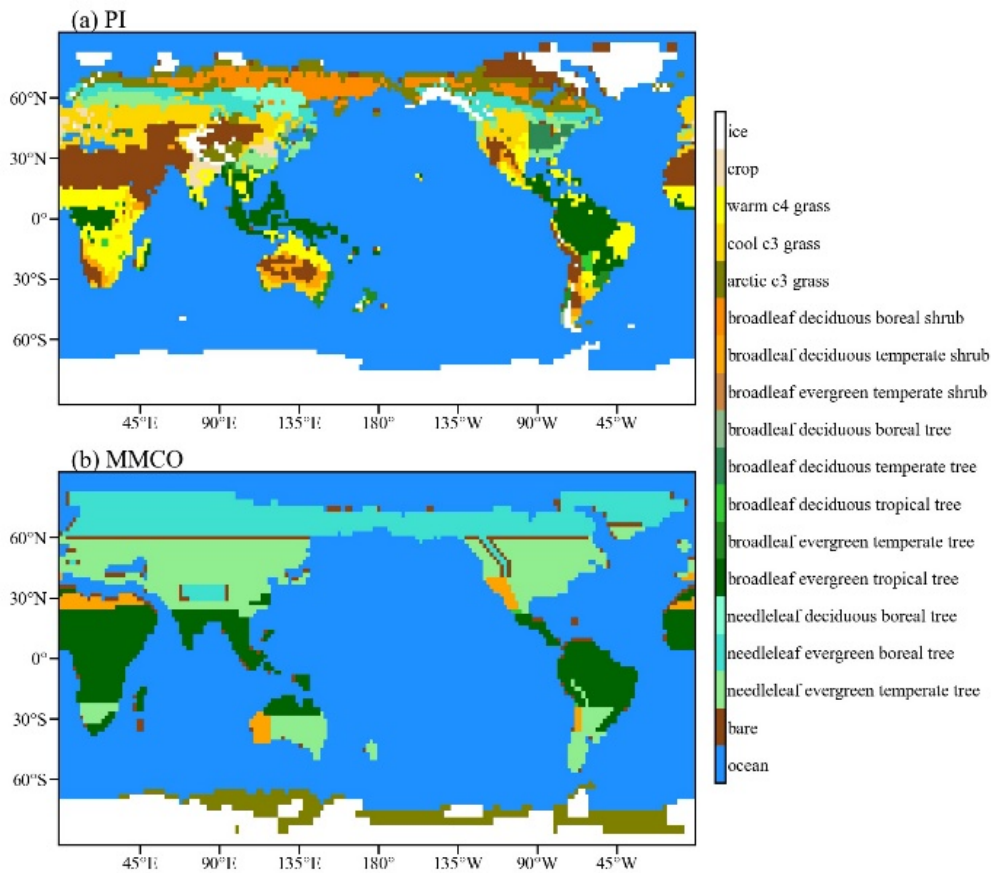


Figure S1. The dominant PFT (Plant Function Type) map for (a) PI and (b) MMCO.

Figure S1 shows the dominant PFT (Plant Function Type) map for (a) PI and (b) MMCO. The dominant PFT means that the percentage of specific PFT in a grid cell is the largest except for the Antarctic. In the Antarctic, if bare ground is the dominant land cover but it accounts less than the percentage of arctic grass, then the arctic grass is present. It should be noted that in the MMCO (b), the percentages of needleleaf evergreen temperate tree and broadleaf deciduous temperate tree are the same as 35% in the mid latitudes (30-60°N/S), representing the “warm mixed forest” in the megabiomes data (Frigola et al., 2018). The percentages of needleleaf evergreen boreal tree and broadleaf deciduous boreal tree are also the same as 35% in the high latitudes (>60°N), representing the “cool mixed forest” in Frigola et al. (2018).

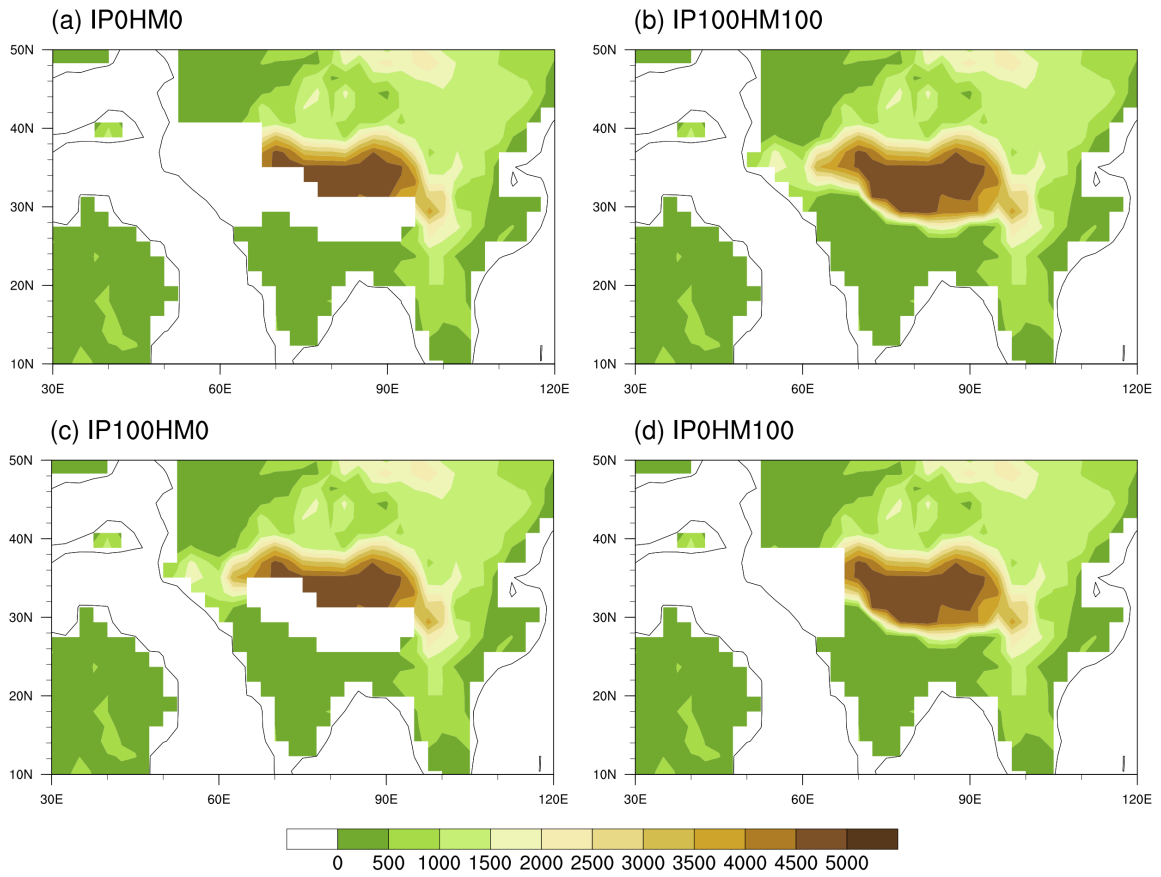


Figure S2. Topography of orographic sensitivity experiments at $1.9^\circ \times 2.5^\circ$ resolution, including (a) IPOHM0, (b) IP100HM100, (c) IP100HM0 and (d) IPOHM100.

SM2: Moisture budget decomposition

The moisture budget is written as:

$$P' = - \langle \omega \partial_p q \rangle' - \langle V \cdot \nabla q \rangle' + E' + \text{residual} \quad (1)$$

Where the angle bracket $\langle \rangle$ means a mass integration through the troposphere, the primes ' represent the difference between experiments with and without the uplift of IP and HM. P and E denote precipitation and evaporation, respectively. V and ω represent horizontal wind and vertical pressure velocity, respectively. And q is specific humidity. $\langle \omega \partial_p q \rangle'$ and $\langle V \cdot \nabla q \rangle'$ represent vertical moisture advection and horizontal moisture advection, respectively, and can be further divided into the thermodynamic and dynamic terms:

$$-\langle \omega \partial_p q \rangle' = -\langle \bar{\omega} \partial_p q' \rangle - \langle \omega' \partial_p \bar{q} \rangle - \langle \omega' \partial_p q' \rangle \quad (2)$$

$$-\langle V_h \cdot \nabla q \rangle' = -\langle \bar{V}_h \cdot \nabla q' \rangle - \langle V_h' \cdot \nabla \bar{q} \rangle - \langle V_h' \cdot \nabla q' \rangle \quad (3)$$

$-\langle \omega' \partial_p \bar{q} \rangle$ and $-\langle V_h' \cdot \nabla \bar{q} \rangle$ are dynamic terms related to changes in circulation, while $-\langle \bar{\omega} \partial_p q' \rangle$ and $-\langle \bar{V}_h \cdot \nabla q' \rangle$ are thermodynamic terms related to changes in specific humidity.

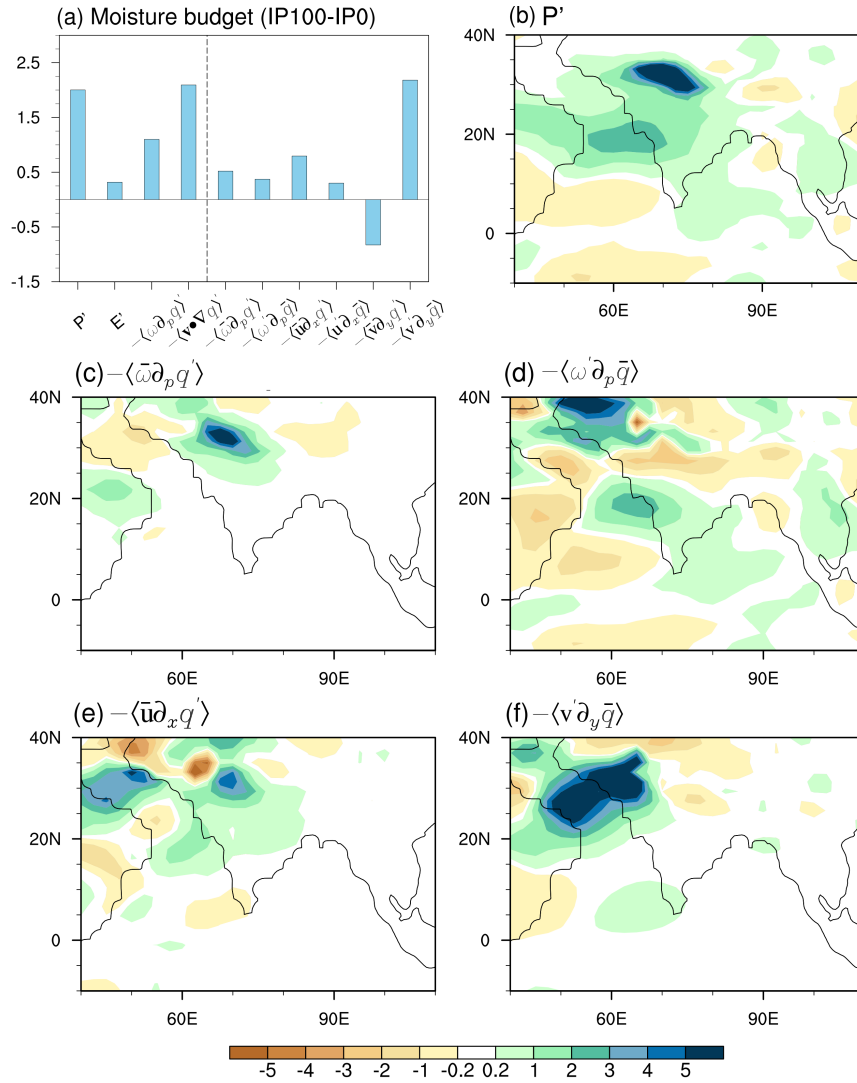


Figure S3. (a) Moisture budget for regional mean precipitation differences (mm day⁻¹) over the west part (15-35°N, 50-75°E) of the South Asian monsoon region between IP100 and IP0 experiments. Spatial distribution of (b) precipitation difference, (c) anomalous vertical moisture advection by climatological vertical motion (thermodynamic term) $-\langle \bar{\omega} \partial_p q' \rangle$; (d) anomalous advection of the climatological vertical moisture by vertical motion anomalies (dynamic term) $-\langle \omega' \partial_p \bar{q} \rangle$; (e) anomalous horizontal moisture advection by climatological zonal wind $-\langle \bar{u} \partial_x q' \rangle$ and (f) anomalous horizontal advection of the climatological moisture by meridional wind anomalies $-\langle v' \partial_y \bar{q} \rangle$.

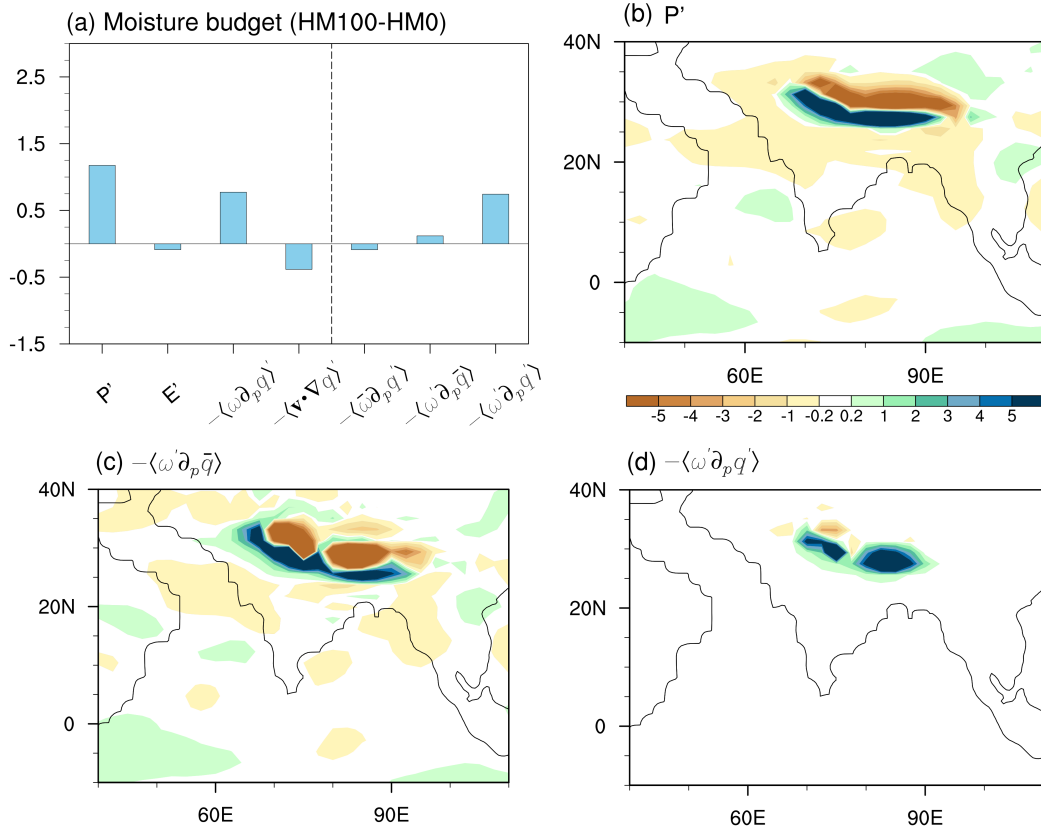


Figure S4. (a) Moisture budget for regional mean precipitation differences (mm day^{-1}) over the east part ($15\text{-}29^\circ\text{N}$, $75\text{-}95^\circ\text{E}$) of the South Asian monsoon region between HM100 and HM0 experiments. Spatial distribution of (b) precipitation difference, (c) anomalous advection of the climatological vertical moisture by vertical motion anomalies (dynamic term) $-\langle \omega' \partial_p \bar{q} \rangle$ and (d) anomalous moisture advection by both vertical motion anomalies and specific humidity anomalies (nonlinear term) $-\langle \omega' \partial_p q' \rangle$.

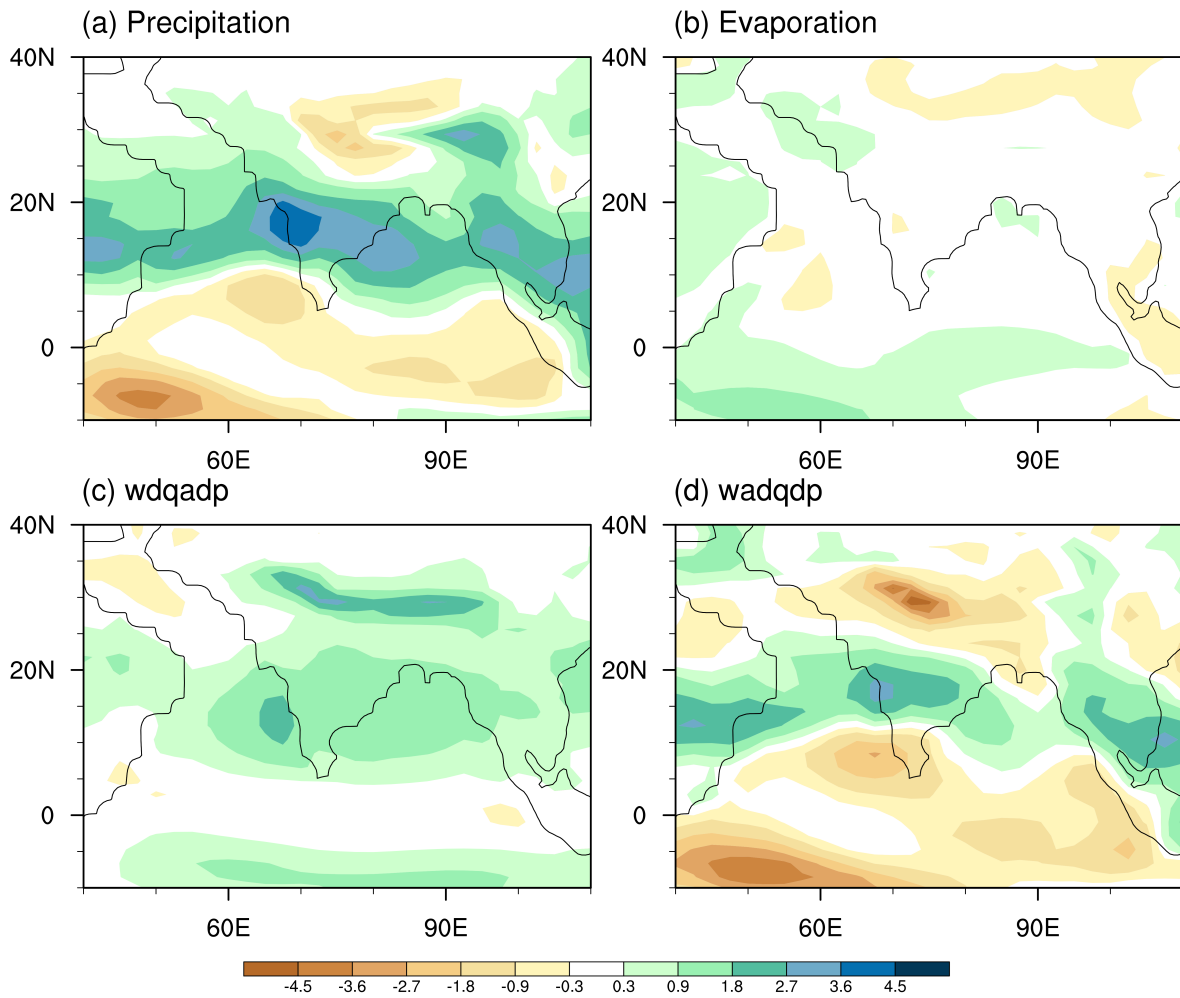


Figure S5. (a) Moisture budget for precipitation differences (mm day^{-1}) between MMIO_1000ppm and MMIO experiments. Spatial distribution of (a) precipitation difference, (b) evaporation, (c) anomalous vertical moisture advection by climatological vertical motion (thermodynamic term) $-\langle \bar{\omega} \partial_p q' \rangle$; (d) anomalous advection of the climatological vertical moisture by vertical motion anomalies (dynamic term) $-\langle \omega' \partial_p \bar{q} \rangle$.

SM3: Geographic sensitivity experiments

In order to test (1) which topography change is responsible to the establish the Somali Jet; (2) if the topographic effect is sensitive to geography, we use the Atmospheric component of CESM1.2 to conduct a series of 5 experiments (Table S1). These simulations are integrated over 50 years starting at the end of previous experiment MMIO. CO₂ is set as 400 ppm; vegetation setting follows geography as modern or Miocene map. Three previous simulations IP0HM0, MMIO and piControl are also list for reason of first-order comparison.

Table S1: List of experiments. Abbreviations stand for Himalaya (HM), Iranian Plateau (IP), Arabian Plateau (ARB) and East African Highlands (EAF). Among them, IP0HM0, MMIO and piControl are simulations with coupled CESM1.2; the others are performed with its atmospheric component only. The height of the IP in MMCO and piControl are the heigh in the Middle Miocene and modern day, respectively.

	Geography	HM(%)	IP(%)	ARB(%)	EAF(%)
Modern_IP0HM0_ARB100_EAF100	modern	0	0	100	100
Modern_IP0HM0_ARB25_EAF100	modern	0	0	25	100
Modern_IP0HM0_ARB25_EAF25	modern	0	0	25	25
MMIO_IP0HM0_ARB100_EAF100	Miocene	0	0	100	100
MMIO_IP0HM0_ARB25_EAF100	Miocene	0	0	25	100
IP0HM0	Miocene	0	0	25	25
MMCO	Miocene	80	100	25	25
piControl	modern	100	100*	100	100

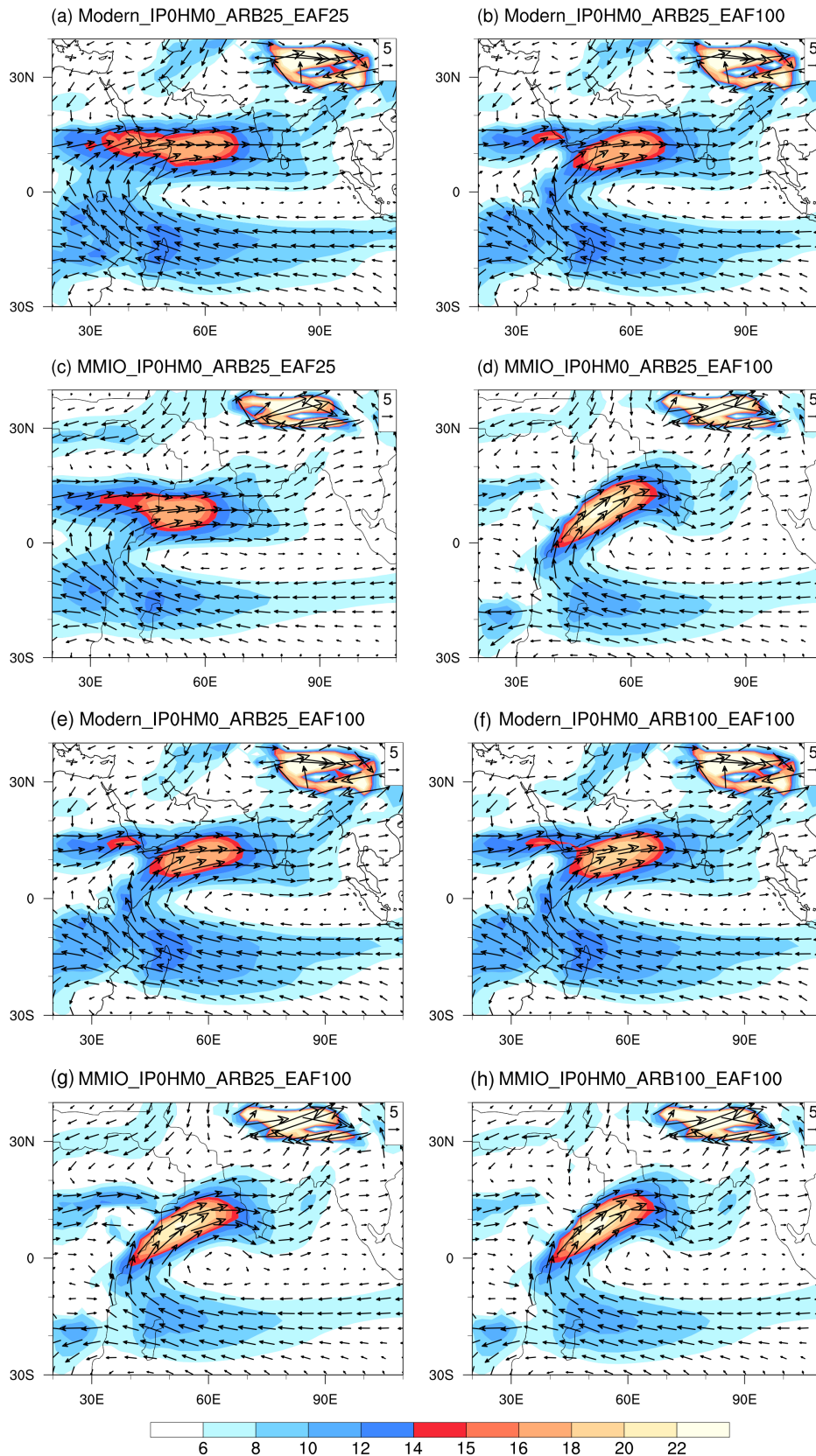


Figure S6. Climatology of JJA (June-July-August) mean 850 hPa winds (vectors, m s^{-1}) over the South Asia summer monsoon (SASM) region in (a) Modern_IP0HM0_ARB25_EAF25, (b)

Modern_IP0HM0_ARB25_EAF100, (c) MMIO_IP0HM0_ARB25_EAF25, (d)
MMIO_IP0HM0_ARB25_EAF100, (e) Modern_IP0HM0_ARB25_EAF100, (f)
Modern_IP0HM0_ARB100_EAF100, (g) MMIO_IP0HM0_ARB25_EAF100, and (h)
MMIO_IP0HM0_ARB100_EAF100 experiments. Shading represents wind speed (units: m s^{-1}). Shading represents wind speed (units: m s^{-1}).

Figure S6 shows that the uplift of the EAF is essential to producing the Somali Jet along the eastern coast of Africa independent the applied geography. In response to the uplift of the Arabian Plateau, the change in atmospheric circulations and associated precipitation is sensitive to the applied geography.

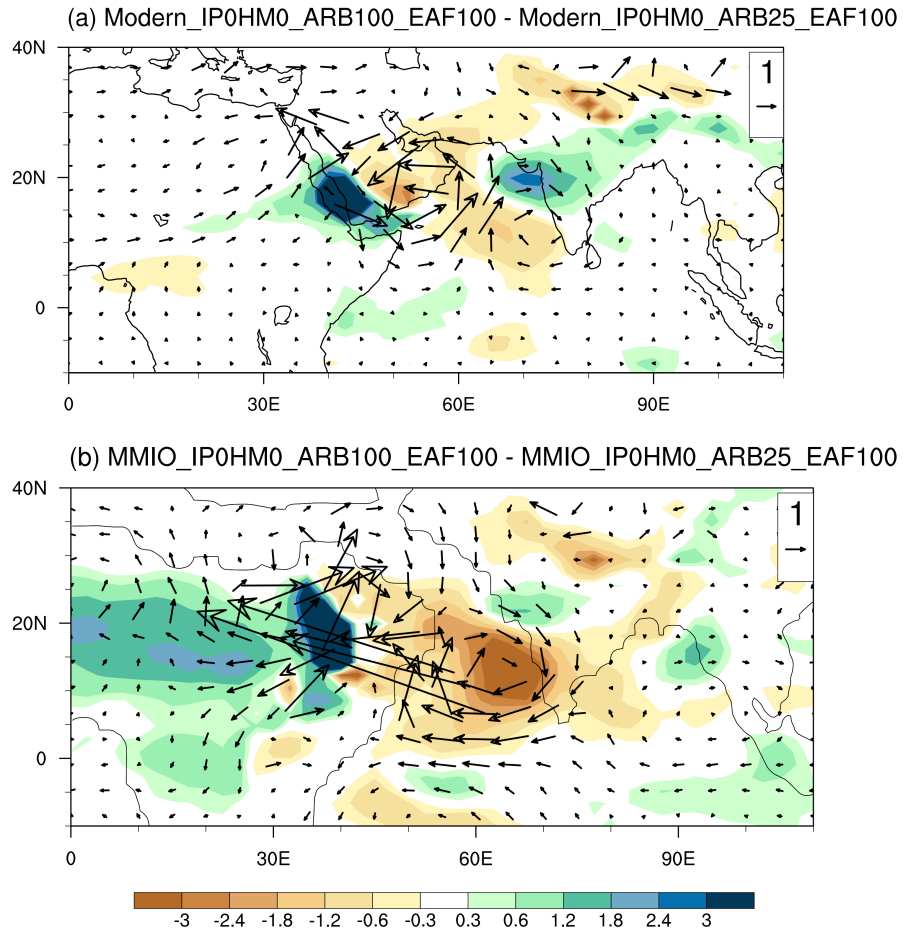


Figure S7. Precipitation (shaded, mm day^{-1}) and 850hPa wind differences between (a) Modern_IP0HM0_ARB100_EAF100 and Modern_IP0HM0_ARB25_EAF100 experiments; (b) MMIO_IP0HM0_ARB100_EAF100 and MMIO_IP0HM0_ARB25_EAF100 experiments.